

The ICARUS Experiment

Inés Gil Botella^{*†}

Institute for Particle Physics, ETH Hönggerberg, CH-8093 Zürich, Switzerland

E-mail: Ines.Gil.Botella@cern.ch

ABSTRACT: The ICARUS experiment consists of an imaging liquid argon Time Projection Chamber (TPC) detector providing high granularity and high accuracy measurements over large sensitive volumes. This multipurpose detector opens up unique opportunities to look for phenomena beyond the Standard Model through the study of atmospheric, solar and supernova neutrinos, nucleon decay searches and neutrinos from the CERN to Gran Sasso beam. A summary of the general physics program and the current status of the ICARUS experiment is reported.

1. Introduction

ICARUS is a project, proposed in 1985 [1], for the installation of a large liquid argon Time Projection Chamber (TPC) in the Gran Sasso laboratory (LNGS) in Italy, for the study of neutrino physics and matter stability. Several years of R&D with prototypes of increasing size have allowed to overcome the major technological problems in the establishment of this technique.

As a first step to reach the final mass of 3000 tons [2], a full scale 600 ton module (T600) has been constructed and tested in 2001 at surface conditions. This liquid argon device has demonstrated the feasibility of the technique and the detector's capability to collect high quality data for physics analyses.

The ability of the LAr TPC to provide 3D imaging of any ionizing event together with an excellent calorimetric response offers the possibility to perform complementary and simultaneous measurements of neutrinos, as those of the CERN to Gran Sasso beam (CNGS), those from cosmic ray events, and even those from the sun and from supernovae. The same class of detector can also be envisaged for high precision measurements at a neutrino factory and can be used to perform background-free searches for nucleon decays. Hence an extremely rich and broad physics program, encompassing both accelerator and non-accelerator physics, will be addressed [3]. These will answer fundamental questions about neutrino properties and about the possible physics of the nucleon decay.

^{*}Speaker.

[†]on behalf of the ICARUS Collaboration

2. The LAr TPC technology

The ICARUS detector is a LAr TPC that combines the detection features of a bubble chamber with the advantage of the electronic read-out. The detection principle of the LAr TPC is based on the fact that in highly purified LAr (less than 0.1 part per billion O_2 equivalent) ionization tracks can be transported practically undistorted by a uniform electric field over distances of meters. Imaging is then provided by an appropriate set of electrodes (wires) continuously sensing and recording signals.

The feasibility of this technology has been demonstrated by an extensive R&D program which includes years of studies with different prototypes and it has reached maturity with the construction and full operation on earth's surface of a 600 ton liquid argon device.



Figure 1: Internal view of the T600 first half-module (left half only).

The T600 (Figure 1) [4] is a large cryostat divided in two identical, adjacent half-modules, each one with internal dimensions $3.6 \times 3.9 \times 19.9 \text{ m}^3$. Each half-module houses an internal detector composed of two TPC's separated by a common cathode. Each TPC is formed by three parallel planes of wires oriented at $0, \pm 60^\circ$ to the horizontal, with a pitch of 3 mm between adjacent wires, positioned along the left and right side walls of the half-module. A high voltage system produces a uniform electric field (500 V/cm) perpendicular to the wire planes, forcing the drift of the ionization electrons (the maximum drift path is 1.5 m). These electrons will induce a signal on the wires near which they are drifting while approaching the different wire planes. By appropriate biasing, the first set of planes can be made non-destructive (*Induction planes*), so that the charge is finally collected in the last plane (*Collection plane*).

Each wire plane provides a two-dimensional projection (*view*) of the event, while the signal timing with respect to the trigger gives the position along the drift direction. Ionization in LAr is accompanied by scintillation light emission. This light is detected by large-surface (8") PMT's immersed in the LAr and can provide an absolute time measurement of the event and an internal trigger signal.

A full test of the T600 experimental set-up on the surface of the earth was carried out in Pavia (Italy) during 2001. Although the test was mainly intended as a technical run, a substantial amount of cosmic ray data was acquired. The ongoing data analysis confirms the excellent detector performances. The muon decay energy spectrum (Figure

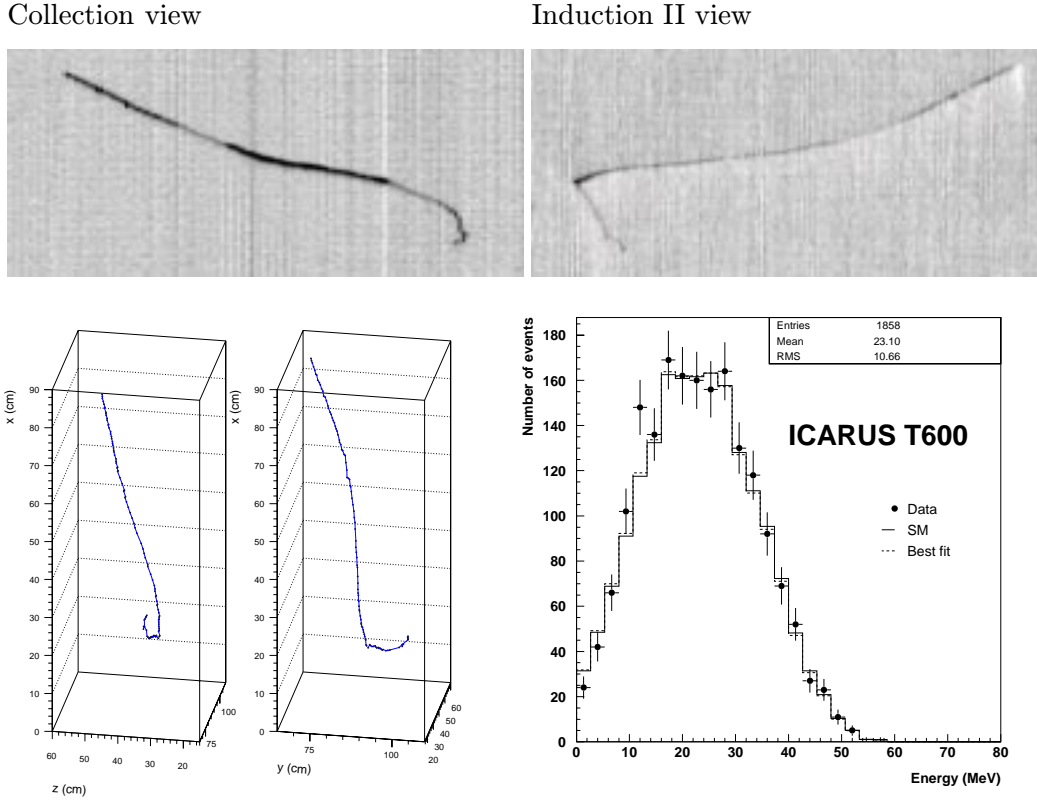


Figure 2: Top: Stopping muon event 2D projection views corresponding to the Collection (left) and Induction II (right) wire planes; Bottom left: 3D full reconstruction of the event; Bottom right: Michel electron spectrum from the stopping muon event sample in the ICARUS T600 detector.

2) has been measured from a sample of stopping muon events acquired during the test run. The obtained result [5] constitutes a proof of the maturity of the detection technique to produce high quality physics results.

The T600 detector is now ready to be transported into the LNGS Hall B. The final design of the detector, ICARUS T3000, will be composed of the T600, two modules of 1200 tons and a muon spectrometer [6], with a total mass of 3000 tons. The full project has been recently approved by INFN and CERN and the T3000 is planned to be commissioned for the first CNGS neutrino beam events in 2006.

3. Proton decay searches

The SuperKamiokande (SK) collaboration has extensively probed classical decay channels (e.g., $p \rightarrow e^+\pi^0$) and the dominant decay mode, $p \rightarrow \bar{\nu}K^+$ according to SUSY Grand Unified Theories. Plans exist to operate a megaton water Čerenkov detector [7] in view of improving current sensitivities for $p \rightarrow e^+\pi^0$ and $p \rightarrow \bar{\nu}K^+$ modes by at least one order of magnitude. However, to unmistakably show the existence of a signal, these experiments have to rely on statistical background subtraction.

A clear advantage and certainly the main strength of the ICARUS technique is, that discovery will be possible down to a single event, thanks to its superb imaging and energy

Channel	Eff. (%)	Backg. (5 kton × year)	τ/B limit (10^{32} yr)	Needed Exposure to reach PDG'02 (kton×yr)
$p \rightarrow \mu^- \pi^+ K^+$	98	0.005	5.7	2.1
$p \rightarrow e^+ \pi^+ \pi^-$	19	0.125	1.1	3.8
$p \rightarrow \pi^+ \bar{\nu}$	42	4	1.2	0.5
$p \rightarrow e^+ \pi^+ (\pi^-)$	30	6	0.7	
$p \rightarrow e^+ (\pi^+ \pi^-)$	16	20	0.2	
$n \rightarrow e^- K^+$	96	0.005	6.9	0.24
$n \rightarrow \mu^- \pi^+$	45	0.12	3.2	1.6
$n \rightarrow e^+ \pi^-$	44	0.04	3.2	2.5
$n \rightarrow \pi^0 \bar{\nu}$	45	2.4	2	2.4
$n \rightarrow \mu^- (\pi^+)$	21	15	0.4	
$n \rightarrow e^+ (\pi^-)$	26	27	0.4	

Table 1: Nucleon decay searches with the ICARUS detector. The table shows the detection signal efficiency for the studied proton and neutron decay channels and the expected number of background events for an exposure of 5 kton × year. The two last columns show the obtained lifetime limit/Branching Ratio at 90% C.L. and the needed exposure to reach the current PDG'02 limits.

resolution capabilities. In addition, a full understanding of the mechanism responsible for proton decay requires a precise measurement of all possible branching ratios. Since ICARUS provides a much more powerful background rejection, it can perform a large variety of exclusive decay modes measurements. Inclusive searches are obviously also possible. Hence, a liquid argon detector is an ideal device, in particular, for those channels that are not accessible to Čerenkov detectors due to the complicated event topology, or because the emitted particles are below the Čerenkov threshold (e.g. K^\pm).

Table 1 shows the signal efficiencies and the estimated number of background events for an exposure of 5 kton × year for different proton and neutron decay channels. The obtained limits on (τ/B) and the value of the needed exposure to reach the current PDG'02 [8] limits are listed in the two last columns. In general, the better limits are obtained on the exclusive channels. The tag based on the presence of a kaon or a pion accompanied by a charged lepton, with total measured energy around the proton mass, is powerful enough to annihilate the background.

4. Atmospheric neutrinos

The physics goals of new atmospheric neutrino measurements are to firmly establish the evidence of neutrino oscillations with a different experimental technique than SK, possibly free of systematic biases, measure the oscillation parameters and clarify the nature of the oscillation mechanism. The capability to observe all separate processes, electron, muon and tau neutrino charged current events (CC) and all neutral currents (NC) without detector biases and down to kinematical threshold is also highly desirable. A detector based on the ICARUS technique will provide an observation of atmospheric neutrinos of a very

	No osci	Δm_{23}^2 (eV ²)			
		5×10^{-4}	1×10^{-3}	3.5×10^{-3}	5×10^{-3}
Muon-like	675 ± 26	515 ± 23	495 ± 22	470 ± 22	455 ± 21
Contained	418 ± 20	319 ± 18	307 ± 18	291 ± 17	282 ± 17
Partially-Contained	257 ± 16	196 ± 14	188 ± 14	179 ± 13	173 ± 13
No proton	260 ± 16	190 ± 14	185 ± 14	170 ± 13	165 ± 13
One proton	205 ± 14	160 ± 13	150 ± 12	145 ± 12	140 ± 12
Multi-prong	210 ± 14	165 ± 13	160 ± 13	155 ± 12	150 ± 12
Electron-like	380 ± 19	380 ± 19	380 ± 19	380 ± 19	380 ± 19
No proton	160 ± 13	160 ± 13	160 ± 13	160 ± 13	160 ± 13
One proton	120 ± 11	120 ± 11	120 ± 11	120 ± 11	120 ± 11
Multi-prong	100 ± 10	100 ± 10	100 ± 10	100 ± 10	100 ± 10
NC	480 ± 22	480 ± 22	480 ± 22	480 ± 22	480 ± 22
TOTAL	1535 ± 39	1375 ± 37	1355 ± 37	1330 ± 36	1315 ± 36

Table 2: Expected atmospheric neutrino rates for 5 kton \times year in case no oscillations occur and assuming $\nu_\mu \rightarrow \nu_\tau$ oscillations with maximal mixing. Four different Δm^2 values have been considered. Only statistical errors are quoted.

high quality, thanks to its unique performances in terms of resolution and precision. The perspective of ICARUS is to provide redundant, high precision measurement and minimize as much as possible the systematics uncertainties of experimental origin which affect the results of existing experiments. Improvements over existing methods are expected in neutrino event selection, identification of ν_μ , ν_e and ν_τ flavors and neutral currents.

The expected atmospheric neutrino rates obtained for an exposure of 5 kton \times year are summarized in Table 2, with and without $\nu_\mu \rightarrow \nu_\tau$ oscillation hypothesis ($\sin^2 2\theta = 1$).

Muon-like events contain an identified muon and correspond to $\nu_\mu/\bar{\nu}_\mu$ CC events. Electron-like are $\nu_e/\bar{\nu}_e$ CC events with an identified electron. Given the clean event reconstruction, the ratio of “muon-like” to “electron-like” events can be determined free of large experimental systematic errors. In fact, the expected purity of the samples is above 99%. In particular, the contamination from π^0 in the “electron-like” sample is expected to be completely negligible.

We split further the muon-like events into contained and partially-contained samples. For the contained events (62% of the total), the muon energy is precisely determined by integration of the dE/dx measurements along the track. For partially contained events (38% of the total, average neutrino energy 4.5 GeV), in which the muon escapes the detector active volume, the muon momentum is estimated via the multiple scattering method. We illustrate also the expected kind of events, classified according to their final state multiplicity. Approximately 40% of muon-like events contain no identified proton with kinetic energy above 50 MeV in the final state, corresponding to the “one-ring” sample. The rest of the events contain a proton or multi-prongs final states, which provide, thanks to the precise reconstruction of all particles, a precise determination of the incoming neutrino energy and direction (for events with $E_{vis} > 1$ GeV).

5. Solar and supernova neutrinos

ICARUS can detect solar and supernova neutrinos through the following processes:

1. Elastic scattering on electrons ($\nu e^- \rightarrow \nu e^-$), which occurs with all types of neutrino flavors and for both charged and neutral exchange
2. Charged-current (CC) interactions on argon ($\nu_e {}^{40}\text{Ar} \rightarrow e^- {}^{40}\text{K}^*$ and $\bar{\nu}_e {}^{40}\text{Ar} \rightarrow e^+ {}^{40}\text{Cl}^*$)
3. Neutral-current (NC) interactions on argon ($\nu {}^{40}\text{Ar} \rightarrow \nu {}^{40}\text{Ar}^*$)

It is possible to separate the various channels by a classification of the associated photons from the K , Cl or Ar de-excitation, which exhibit specific spectral lines, or by the absence of associated photons in case of the elastic scattering.

Small prototypes have demonstrated that, by the TPC technique, electrons with kinetic energy as low as 150 KeV can be detected [9]. This performance allows a detailed reconstruction of the neutrino interactions. However, because of the increasing backgrounds at low energy, there is a minimum threshold (5 MeV) below which electrons produced by solar neutrinos can not be distinguished from other sources. Our detector is sensitive to the ${}^8\text{B}$ and ${}^{\text{hep}}$ part of the solar neutrino spectrum. For primary electron energies larger than 5 MeV, 3240 solar neutrino events per kton \times year are expected in case of no oscillations.

The most dangerous source of background for solar neutrinos able to generate electrons above the considered energy threshold are neutrons. They come from the natural radioactivity of the rock surrounding the detector in the Gran Sasso laboratory and from radioactive contamination of the structural materials.

A good separation between signal and background events can be achieved considering the electron and photons energy correlation. Figure 3 (left) shows the distribution of the leading cluster energy versus the energy of the photons present in the solar neutrino events. We can easily distinguish the elastic events, with photons energy almost zero, from the absorption events. Colors correspond to the number of events expected in the T600 fiducial volume per year. A similar plot for background events is shown in Figure 3 (right), where numbers correspond to $\sqrt{\text{events}}$ per year in the T600. The contribution from neutron captures on ${}^{40}\text{Ar}$ is located at lower energies while captures on ${}^{36}\text{Ar}$ are at higher energies. We also see the correlation between both variables due to the fact that the total visible energy in the event is fixed. For visible energies larger than 8.8 MeV no background from neutron captures on Ar is expected and a total of 500 solar neutrino events per year can be detected in a 600 ton ICARUS module.

The ICARUS detector has also high capabilities to observe neutrinos from stellar collapses and extract information about their properties [10]. Supernovae and neutrino physics can be studied by the simultaneous observation of NC, ν_e CC, $\bar{\nu}_e$ CC and elastic channels. The matter effects inside the supernova must be included to predict how the spectra of the neutrino burst is modified by oscillations. Observations of the neutrino spectra from supernovae will allow to determine the nature of the mass hierarchy, i.e., normal or inverted and to probe the neutrino mixing angle θ_{13} .

ahhep2003

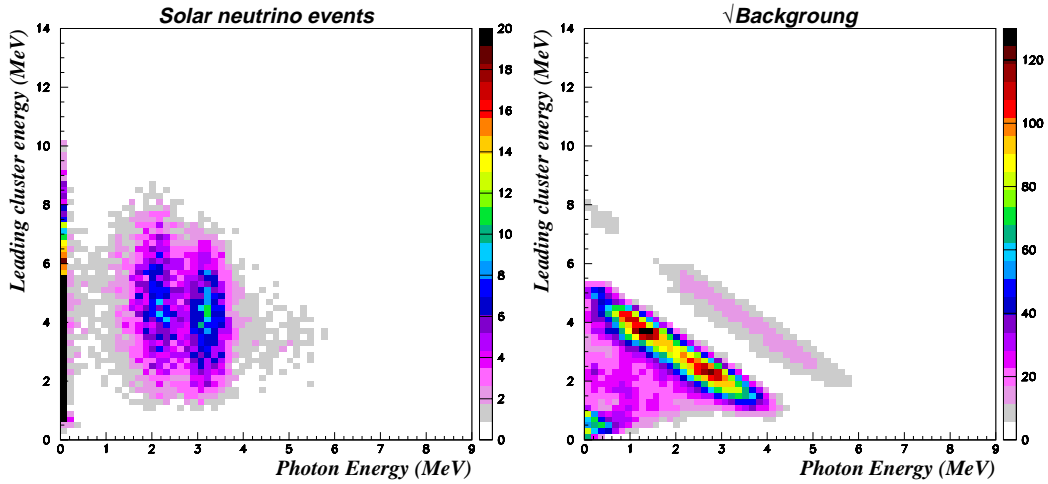


Figure 3: Distribution of the expected solar neutrino events per year (left) and neutron capture events per year (right) in the T600 fiducial volume in the plane of the electron and associated photons energy.

Reaction		No oscillation	Oscillation (n.h.)		Oscillation (i.h.)	
			Large θ_{13}	Small θ_{13}	Large θ_{13}	Small θ_{13}
Elastic	νe^-	41	41	41	41	41
CC	$\nu_e {}^{40}\text{Ar}$	188	962	730	730	730
	$\bar{\nu}_e {}^{40}\text{Ar}$	15	33	33	75	33
NC	$\nu {}^{40}\text{Ar}$	911	911	911	911	911
Total		1155	1947	1715	1757	1715

Table 3: Expected supernova neutrino events in a 3 kton LAr detector including neutrino oscillations with matter effects inside the supernova. The flux parameters are $\langle E_{\nu_e} \rangle = 11$ MeV, $\langle E_{\bar{\nu}_e} \rangle = 16$ MeV, $\langle E_{\nu_{\mu,\tau}} \rangle = \langle E_{\bar{\nu}_{\mu,\tau}} \rangle = 25$ MeV and luminosity equipartition among flavors is assumed.

Table 3 contains the number of neutrino events expected in a 3 kton LAr detector from a supernova with total binding energy of 3×10^{53} ergs at 10 kpc. Elastic, CC and NC processes have been considered independently and oscillation and non oscillation cases have been computed for normal (n.h.) and inverted (i.h.) hierarchies. Two limiting cases depending on the value of the θ_{13} parameter are considered: small θ_{13} which corresponds to $\sin^2 \theta_{13} < 2 \times 10^{-6}$ and large θ_{13} for $\sin^2 \theta_{13} > 3 \times 10^{-4}$. We assume that the energy spectra of neutrinos is a Fermi-Dirac distribution with average energies $\langle E_{\nu_e} \rangle = 11$ MeV, $\langle E_{\bar{\nu}_e} \rangle = 16$ MeV, $\langle E_{\nu_{\mu,\tau}} \rangle = \langle E_{\bar{\nu}_{\mu,\tau}} \rangle = 25$ MeV and luminosity equipartition among flavors. In this kind of scenario where the energies are rather different (hierarchical) between flavors, the effect of the oscillation is very pronounced. Indeed, oscillations will harden the ν_e spectrum, as expected, which has a big incidence of the ν_e CC channel.

The number of observed ν_e can distinguish between the non oscillation case, the n.h.-L case, with an enhancement of a factor 5, and the three other oscillation scenarios (factor 4 increase). A roughly factor 5 enhancement of observed $\bar{\nu}_e$ CC would be a clear indication for

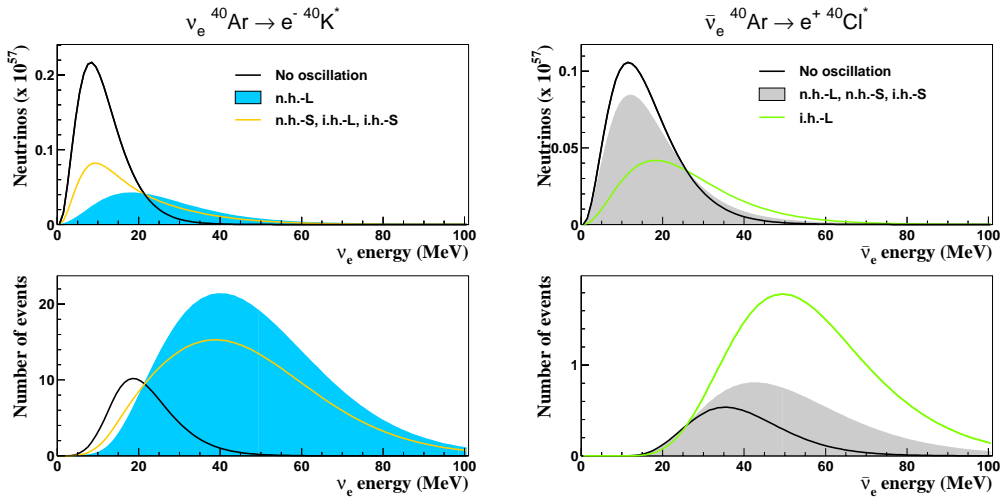


Figure 4: Number of ν_e (left) and $\bar{\nu}_e$ (right) neutrinos arriving at Earth from a supernova at 10 kpc (top) and expected number of ν_e CC (left) and $\bar{\nu}_e$ CC (right) events in a 3 kton LAr detector (bottom).

an oscillation matter enhancement only possible in the inverted mass hierarchy with large mixing angle. Otherwise, a roughly factor 2 enhancement is expected from the effect of oscillations. The neutral current events are not affected by oscillations and they constitute an excellent probe for the supernova properties independent of the neutrino oscillation intrinsic properties.

Figures 4 show the oscillation effects in the neutrino energy spectra. The plots on the top correspond to the expected number of neutrinos arriving at Earth and the bottom plots show the number of events detected in a 3 kton LAr detector. The four oscillation cases are considered in the distributions. Due to the total conversion $\nu_{\mu,\tau} \rightarrow \nu_e$ for the n.h.-L case, the ν_e energy spectra is harder and this leads a huge increase of the expected events due to the quadratic dependence of the CC cross section with energy. The same effect can be seen for $\bar{\nu}_e$ events and i.h.-L case. The elastic processes are less sensitive to the oscillations and smaller number of events is expected. Nevertheless, the energy spectrum is modified specially for $\nu_{\mu,\tau}$ events, moving to lower values of energy due to the neutrino mixing.

Figure 5 shows the the variation of the neutrino rates as a function of $\sin^2 \theta_{13}$. We compare the expected results for the cases of n.h. (solid line), i.h. (dotted line) and no oscillation (dashed line). CC events are very sensitive to the change on the energy spectra due to oscillations. A clear increase on the number of events is expected, being of a factor (4-5) for ν_e CC events and a factor 2 for $\bar{\nu}_e$ CC interactions. The number of ν_e CC events increases 30% from small to large θ_{13} values and $\bar{\nu}_e$ CC events are doubled. Small variations are expected for the rest of channels.

ICARUS can also detect neutrinos coming from the early phase of the supernova core collapse evolution mainly through the CC process. The prompt electron neutrino burst is in principle observable and represents a diagnostic of the fundamental collapse supernova behavior. The characteristic time of the breakout burst is of the order of tens of ms [11].

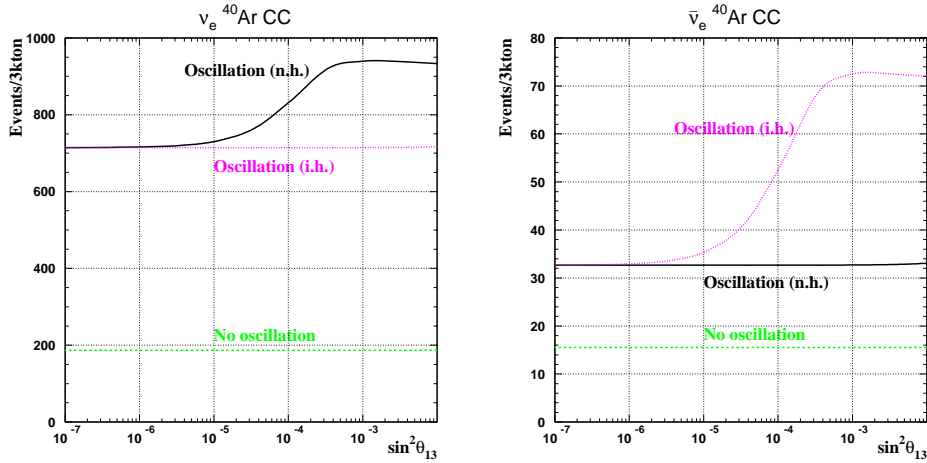


Figure 5: Expected number of supernova neutrino events in a 3 kton LAr detector as a function of $\sin^2\theta_{13}$ for ν_e CC and $\bar{\nu}_e$ CC processes. Solid lines correspond to the n.h. oscillation case, dotted lines to the i.h. case and dashed lines to the non oscillation case.

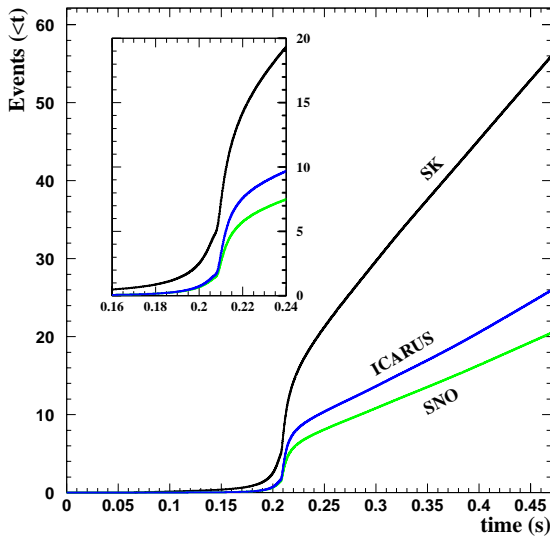


Figure 6: Comparison of the expected number of events from the ν_e breakout burst of a supernova at 10 kpc in a 3 kton ICARUS, SK and SNO experiments.

Neutrino oscillations modify dramatically the flavor content of the neutrinos emitted from the supernova during the burst. The suppression of the ν_e flavor is maximal in the case of normal mass hierarchy and large θ_{13} mixing angle. The expected flux is reduced in a factor 4-3 compared to the non oscillation case. Therefore, it will be difficult to study

Figure 6 compares the integrated number of ν_e events from the break-out burst as a function of time for SK, SNO and ICARUS without including oscillation effects. A total of 10 events are expected in the 3 kton ICARUS in the 40 ms after the bounce: 8 events from the CC channel and 2 from the elastic channel. The contribution of SK and SNO for the same interval of time is 20 and 7 events, respectively.

The event statistics that would be obtained in SK, SNO and the 3 kton ICARUS are similar. In this case, SNO and ICARUS benefit largely from their direct sensitivity to ν_e via charged current interactions on resp. deuteron and Argon, while in SK one has to rely on elastic scattering on

electrons, which has a much smaller cross-section. Hence, smaller detectors like SNO and ICARUS can compare favorably with the largest SK in the study of the breakout phase.

Neutrino oscillations modify dramatically the flavor content of the neutrinos emitted from the supernova during the burst. The suppression of the ν_e flavor is maximal in the case of normal mass hierarchy and large θ_{13} mixing angle. The expected flux is reduced in a factor 4-3 compared to the non oscillation case. Therefore, it will be difficult to study

the neutrino burst within the current round of experiments given the reduction of statistics following the conversion of ν_e into other flavors. In the context of the LAr TPC, a 70 kton detector will be mandatory in order to collect sufficient events to study the neutrino burst.

6. CNGS neutrino beam

In the CERN-NGS beam [12], the expected ν_e and ν_τ contamination are of the order of 10^{-2} and 10^{-7} respectively compared to the dominant ν_μ composition. These properties allow to search for oscillations by looking at the appearance of ν_e or ν_τ charged current events. In this case, the detector must be able to tag efficiently the interaction of ν_e 's and ν_τ 's out of the bulk of ν_μ events. This requires a detailed event reconstruction that can be achieved only by means of a high granularity detector. This requirement is met by the liquid argon target.

To search for the appearance of ν_τ , we exploit the excellent electron measurement and identification capabilities available in ICARUS and concentrate on the $\tau \rightarrow e\nu\nu$ decay mode. Because of the high resolution on measuring kinematical quantities, the ν_τ appearance search is based on the kinematical suppression of the background. To reconstruct the hadronic jet, the detector is used as an homogeneous calorimeter. We expect the main background of the intrinsic ν_e CC component of the beam to be suppressible to a few events, while keeping a $\approx 30\%$ efficiency for the signal. The expected number of ν_τ CC with $\tau \rightarrow e\nu\nu$ for $\Delta m^2 = 3.5 \times 10^{-3} \text{ eV}^2$ is $\simeq 70$ events in five years of “shared” running (equivalent to $5 \times 4.5 \times 10^{19}$ pots), while the background from $\nu_e, \bar{\nu}_e$ CC amounts to about 290 events, or a signal over background $S/\sqrt{B} = 4$.

To enhance the τ appearance sensitivity, we adopt a multi-dimensional likelihood function. This approach offers the advantage of taking into account correlations between the chosen variables, hence, yielding a better separation between signal and background. Assuming five CNGS “shared” years of operation, we expect 13 taus and less than one event of background.

The hadronic decays of the τ can be used to search for $\nu_\mu \rightarrow \nu_\tau$ oscillations, as well. To enhance our sensitivity, we consider two orthogonal event samples: deep-inelastic (DIS) events, with an energetic hadronic jet and large final state multiplicity and quasi-elastic (QE) events, with a very soft hadronic system and small final state multiplicity. For an overall tau efficiency of 1.6%, we expect 2 $\tau \rightarrow \rho$ DIS candidates and a negligibly small

τ decay mode	Signal	Signal	Signal	Signal	BG
	$\Delta m^2 =$ $1.6 \times 10^{-3} \text{ eV}^2$	$\Delta m^2 =$ $2.5 \times 10^{-3} \text{ eV}^2$	$\Delta m^2 =$ $3.0 \times 10^{-3} \text{ eV}^2$	$\Delta m^2 =$ $4.0 \times 10^{-3} \text{ eV}^2$	
$\tau \rightarrow e$	3.7	9	13	23	0.7
$\tau \rightarrow \rho$ DIS	0.6	1.5	2.2	3.9	< 0.1
$\tau \rightarrow \rho$ QE	0.6	1.4	2.0	3.6	< 0.1
Total	4.9	11.9	17.2	30.5	0.7

Table 4: Expected number of τ and background events collected by 5 T600 modules in five years of “shared” data taking. Signal events correspond to full mixing and four different Δm^2 .

background contamination. For the second sample, 2 $\tau \rightarrow \rho$ QE events and negligible background are estimated, with 1.4% tau efficiency.

The results of the $\nu_\mu \rightarrow \nu_\tau$ appearance searches are summarized in Table 4. It displays the expected signal and background events for 5 T600 modules and five years of “shared” CNGS operation. When combined electron and rho decay channels, 17 taus are expected for a total estimated background smaller than one event. Therefore, the ICARUS sensitivity to the $\nu_\mu \rightarrow \nu_\tau$ oscillations is similar to that of the dedicated OPERA experiment [13].

The excellent electron identification allows to look for electron excess coming from $\nu_\mu \rightarrow \nu_e$ oscillations. At high energy, we cannot neglect in addition the $\nu_\mu \rightarrow \nu_\tau$ oscillations with $\tau \rightarrow e\nu\nu$ to distort the electron sample. We adopt an approach in which both $\nu_\mu \rightarrow \nu_e$ and $\nu_\mu \rightarrow \nu_\tau$ oscillations are fitted simultaneously. A kinematical analysis is used to separate the two contributions.

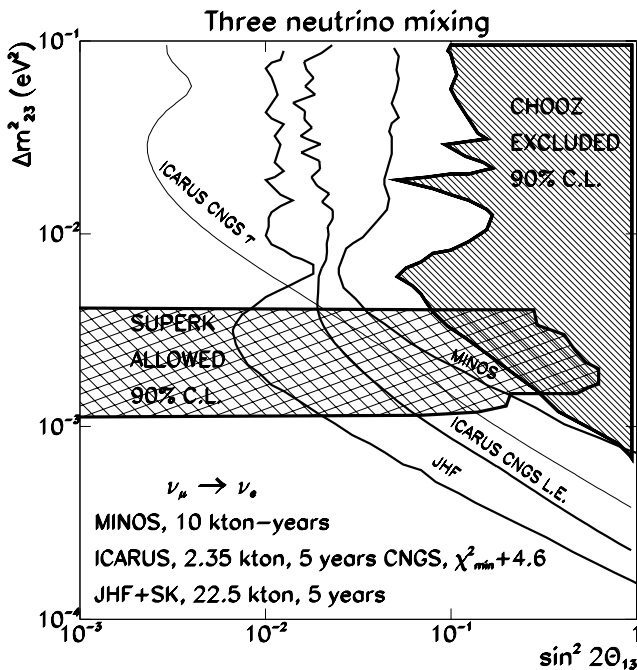


Figure 7: Sensitivity to the parameter θ_{13} at the 90% C.L. ($\chi^2_{min} + 4.6$, 2 parameter C.L.) in a three family mixing scenario, in presence of $\nu_\mu \rightarrow \nu_\tau$ oscillations with $\theta_{23} = 45^\circ$.

case, the mixing angle between ν_μ and ν_τ was set to $\theta_{23} = 45^\circ$. Clearly, for high Δm_{32}^2 values, the improvement with respect to CHOOZ is almost two orders of magnitude. For $\Delta m_{32}^2 = 3 \times 10^{-3} \text{ eV}^2$, the limit could be improved by more than a factor 6.

7. Conclusions

The liquid argon TPC technology has come to maturity with the full operation of the first 600 ton module in a test run at surface. The analysis of the huge amount of data acquired is showing the excellent capabilities of the detector.

In order to disentangle $\nu_\mu \rightarrow \nu_e$ and $\nu_\mu \rightarrow \nu_\tau$ oscillations, we considered the transverse missing momentum. The $\nu_\mu \rightarrow \nu_e$ events are balanced, while $\nu_\mu \rightarrow \nu_\tau$ show a sizable transverse momentum due to the presence of two neutrinos in the final state. The visible energy, the missing transverse momentum and the electron transverse momentum are combined into a binned χ^2 -fit, in which the three oscillations parameters Δm_{32}^2 , θ_{23} and θ_{13} are allowed to vary.

The sensitivity to θ_{13} in presence of $\nu_\mu \rightarrow \nu_\tau$ oscillations, which play in this case the role of background, was estimated with the χ^2 method. The 90% C.L. exclusion region, obtained with $\chi^2_{min} + 4.6$ (2 parameter C.L.) for $\sin^2 2\theta_{13}$ is shown in Figure 7 [14]. In this

A broad physics program, including accelerator and non-accelerator physics, will be addressed by ICARUS in the next years, starting early in 2004 with the installation of the first T600 module in the underground Gran Sasso laboratory. The first phase of the program will include the detection of atmospheric and solar neutrino events, supernovae and the search for proton decay with a background-free technique.

On the basis of the experience of the T600 module, the design and assembly of “clones” of the present prototype in a series of units together with the construction of a magnetic muon spectrometer will allow to reach the multi-kton program, for the time of arrival of the CNGS beam, with a mass of the order of 3000 tons.

References

- [1] ICARUS Collaboration, *ICARUS-I: a proposal for the Gran Sasso Laboratory*, INFN/AE-85/7, Frascati (Italy), 1985.
- [2] ICARUS Collaboration, *The ICARUS Experiment: A Second-Generation Proton Decay Experiment and Neutrino Observatory at the Gran Sasso Laboratory*, CERN/SPSC 2002-027 (SPSC-P-323), LNGS-EXP 13/89 add.2/01.
- [3] ICARUS Collaboration, *The ICARUS Experiment: A Second-Generation Proton Decay Experiment and Neutrino Observatory at the Gran Sasso Laboratory*, Proposal Vol. I & II, LNGS-94/99, 1994.
- [4] ICARUS Collaboration, S. Amoruso *et al.*, *Design, construction and tests of the ICARUS T600 detector*. In preparation.
- [5] ICARUS Collaboration, S. Amoruso *et al.*, *Measurement of the muon decay spectrum with the ICARUS T600 liquid Argon TPC*, submitted to *Eur. Phys. J. C*, [hep-ex/0311040](#).
- [6] ICARUS Collaboration, *A magnetized muon spectrometer for ICARUS T3000 at the LNGS/CNGS*, CERN/SPSC 2003-030 (SPSC-P-323-Add.1), LNGS-EXP 13/89 add. 3/03.
- [7] C. K. Jung, *Feasibility of a next generation underground water Cherenkov detector: UNO*, NNN99 at Stony Brook, [hep-ex/0005046](#).
- [8] K. Hagiwara *et al.*, *Phys. Rev. D* **66** (2002) 010001.
- [9] ICARUS Collaboration, *The ICARUS 50 l LAr TPC in the CERN ν Beam*, Proceedings of 36th Workshop On New Detectors, Erice, Italy, 1997, *World Scientific* (1999) 3.
- [10] I. Gil-Botella and A. Rubbia, *Oscillation effects on supernova neutrino rates and spectra and detection of the shock breakout in a liquid argon TPC*, *J. Cosmol. Astropart. Phys.* JCAP **10** (2003) 009, [hep-ph/0307244](#).
- [11] T.A. Thompson, A. Burrows and P.A. Pinto, *Shock Breakout in Core-Collapse Supernovae and its Neutrino Signature*, *Astrophys. J.* **592** (2003) 434-456, [astro-ph/0211194](#).
- [12] G. Acquistapace *et al.*, *The CERN Neutrino beam to Gran Sasso (NGS)*, Conceptual Technical Design, CERN 98-02, INFN/AE-98/05.
- [13] OPERA Collaboration, *Status Report of the OPERA Experiment*, CERN/SPSC 2001-025 (SPSC/M668), LNGS-EXP 30/2001 add.1/01.
- [14] A. Rubbia and P.Sala, *A low energy optimization of the CERN-NGS neutrino beam for a θ_{13} driven neutrino oscillation search*, *J. High Energy Phys.* **09** (2002) 004.